

# Ultrashort-laser-pulse amplification in a XeF( $C \rightarrow A$ ) excimer amplifier

T. E. Sharp, Th. Hofmann, C. B. Dane, W. L. Wilson, Jr., F. K. Tittel, and P. J. Wisoff

Department of Electrical and Computer Engineering, Rice University, P.O. Box 1892, Houston, Texas 77251

G. Szabó

Department of Optics and Quantum Electronics, Jate University, Szeged, Hungary

Received August 27, 1990; accepted October 2, 1990

Tunable blue-green subpicosecond laser pulses have been amplified in an electron-beam-pumped XeF( $C \rightarrow A$ ) excimer amplifier. Small-signal gains of  $3.5\% \text{ cm}^{-1}$  were measured using a 50-cm active gain length. At output energy densities as high as  $170 \text{ mJ/cm}^2$ , only a small degree of saturation occurred, resulting in a gain of  $2.5\% \text{ cm}^{-1}$ .

An ultrashort-laser-pulse amplifier should have a broad and uniform bandwidth, a high capacity for energy storage, and a low level of amplified spontaneous emission (ASE). XeCl and KrF excimer amplifiers have been extensively studied and utilized as ultrashort-laser-pulse amplifiers in the ultraviolet.<sup>1-7</sup> These systems, however, have a limited bandwidth ( $<5 \text{ nm}$ ) and a large cross section for stimulated emission, resulting in low saturation thresholds ( $E_{\text{sat}} \approx 1\text{--}2 \text{ mJ/cm}^2$ ) and high ASE levels. Other ultrashort-laser-pulse amplifier media such as dyes and solid-state materials are limited in performance by induced nonlinear effects at high intensities. Although this limitation has been largely circumvented by the use of chirped-pulse amplification,<sup>8</sup> this technique is still restricted by the bandwidth region over which the chirped pulse can be amplified as well as by the difficulty in scaling the condensed media amplifiers (or compressor components such as gratings) to large apertures. In this Letter we report an alternative approach: to amplify subpicosecond laser pulses in an electron-beam-pumped XeF( $C \rightarrow A$ ) excimer amplifier. Unlike the XeCl and KrF( $B \rightarrow X$ ) amplifiers, the XeF( $C \rightarrow A$ ) excimer transition has a broad bandwidth in the visible spectrum and, owing to its relatively low gain, exhibits both a high energy saturation threshold and low ASE.

Extensive research on electron-beam-pumped XeF( $C \rightarrow A$ ) lasers has resulted in efficient operation by injection seeding with nanosecond laser pulses.<sup>9,10</sup> When the XeF( $C \rightarrow A$ ) laser is not injection seeded but allowed to oscillate freely, strong modulation of the spectrum is apparent owing to absorbing species, primarily metastable Xe and Ar atoms. The shape of the spectrum is also affected by broadband absorption, mainly owing to photoionization of excited Xe atoms. Figure 1 provides an illustrative comparison of the fluorescence spectrum of the XeF( $C \rightarrow A$ ) amplifier with the spectrum of the free-running laser. The fluorescence spectrum has a bandwidth of  $\sim 70 \text{ nm}$ , which, assuming that it could be fully used for amplification, would allow amplification of pulses as short as 5 fsec. It was recently demonstrated that,

owing to the low gain cross section of the XeF( $C \rightarrow A$ ) transition, the absorbers can be saturated before the gain by building up large intensities in the optical field.<sup>9</sup> Injection seeding to exceed the saturation limit of the absorbers was shown to lead to a relatively smooth output power profile as a function of the injection wavelength. By tailoring the gas mixture to minimize absorption in the blue-green and to suppress the  $B \rightarrow X$  transition at 353 nm, a nanosecond laser-injection-controlled XeF( $C \rightarrow A$ ) amplifier can operate with an efficiency of  $\sim 2\%$  and an output energy density of  $2 \text{ J/L}$ .<sup>10</sup>

An important aspect of the excitation of the XeF( $C \rightarrow A$ ) amplifier is that a short-pulse (10 nsec) electron beam is used to pump the system. The  $C$ -state lifetime in the excited gas medium is several times longer than the pumping time, permitting efficient population of the  $C$  state in the afterglow regime of the excitation pulse. In conventional XeCl and KrF discharges, the lifetime of the upper state is too short to convert fully the pumping energy into the desired population inversion. Furthermore, in the electron-beam-

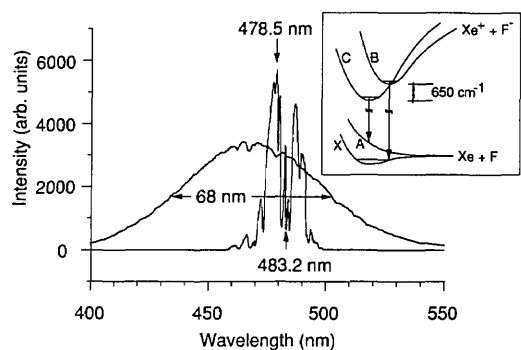


Fig. 1. Spectra of the XeF( $C \rightarrow A$ ) fluorescence and the free-running laser. The absorption lines in the free-running laser are primarily due to excited atomic species created by the electron-beam excitation. The inset shows the relevant energy levels of the XeF excimer. The  $C \rightarrow A$  and  $B \rightarrow X$  laser transitions are indicated. The cross section for stimulated emission for the  $C \rightarrow A$  transition is  $\sim 1 \times 10^{-17} \text{ cm}^2$ , compared with  $\sim 3 \times 10^{-16} \text{ cm}^2$  for the  $B \rightarrow X$  transition.

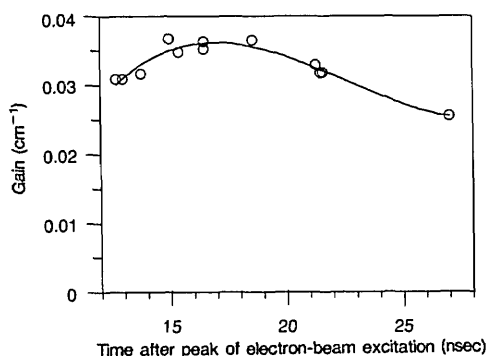


Fig. 2. Temporal peak of the  $\text{XeF}(C \rightarrow A)$  gain at 478.5 nm after electron-beam excitation. The peak of the electron-beam excitation occurs at 0 nsec. The pulse duration of the probe beam was 800 fsec, and the energy flux was  $20 \text{ mJ/cm}^2$ .

pumped  $\text{XeF}(C \rightarrow A)$  amplifier, the vibrational temperature of the  $C$  state is  $\sim 300 \text{ K}$  (Ref. 11) owing to the presence of a high-pressure (6.5 bars) argon buffer atmosphere, i.e., most of the population is relaxed into the lowest vibrational levels. In  $\text{XeCl}$  and  $\text{KrF}$  excimer discharges, the vibrational level populations are not fully relaxed and cannot be equilibrated on the time scale of the passage of the ultrashort pulse through the amplifier. As a result, lower gain is measured in the ultrashort (subpicosecond) regime compared with that observed for nanosecond-length pulses.<sup>1</sup> Amplification of ultrashort laser pulses with the  $\text{XeF}(C \rightarrow A)$  amplifier, however, should be similar to that observed with a nanosecond-pulse injection.

To investigate the amplification of subpicosecond laser pulses, a broadly tunable millijoule blue-green dye-laser system was constructed.<sup>12</sup> This system consists of a hybrid synchronously pumped dye oscillator with the output amplified in a two-stage dye amplifier. The oscillator is pumped with the third harmonic of a cw mode-locked Nd:YAG laser, and the dye amplifiers are pumped with the third harmonic of the regeneratively amplified Nd:YAG laser output. The new two-stage dye amplifier design<sup>12</sup> produced tunable,  $\sim 2\text{-mJ}$ , 850-fsec laser pulses with an ASE content of less than 0.1% for injection into the  $\text{XeF}(C \rightarrow A)$  amplifier.

The temporal peak of the measured single-pass gain of the  $\text{XeF}(C \rightarrow A)$  amplifier at 478.5 nm is given in Fig. 2. The 478.5-nm wavelength corresponds to a peak in the output of the free-running spectrum of the  $\text{XeF}(C \rightarrow A)$  laser as shown in Fig. 1. The gain was measured by comparing simultaneous measurements of the probe pulse and the amplified probe pulse using two calibrated vacuum photodiodes and carefully calibrated beam splitters and neutral-density filters. In addition, the highest output energies were directly confirmed with an energy meter (Moletron). The peak small-signal gain was  $3.5\% \text{ cm}^{-1}$ , which is comparable with the peak small-signal gains measured in earlier nanosecond-pulse probe experiments.<sup>10</sup> Reduction in the gain due to polarization of the probe beam was not observed. This is consistent with the duration of the probe pulses being on the order of the rotational reorientation time, which is estimated to be 0.8 psec by using the 0.28-nm internuclear distance of

the  $\text{XeF}(B)$  state.<sup>13</sup> In addition, as shown in Fig. 2, the gain was greater than  $3\% \text{ cm}^{-1}$  for more than 10 nsec, allowing future multipass experiments to optimize energy extraction from an electron-beam-pumped  $\text{XeF}(C \rightarrow A)$  amplifier.

Figure 3 shows a plot of the single-pass gain as a function of the injected energy density at 478.5 nm. The solid curve represents a Frantz-Nodvik curve<sup>14</sup> that corresponds to a saturation energy of  $120 \text{ mJ/cm}^2$ . Since the absorption cross sections of the identified saturable absorbers are typically 3 to 4 orders of magnitude larger than the stimulated-emission cross section of the  $\text{XeF}(C \rightarrow A)$  transition,<sup>15</sup> the absorbers are expected to be fully saturated at injection energies below the energy scale of Fig. 3; therefore, we believe that the Frantz-Nodvik line provides at least a qualitative description of the gain saturation even though the model generally does not allow for the presence of saturable absorbers. Since the questions related to the applicability of the Frantz-Nodvik model could be fully resolved only on the basis of better knowledge of the absorbers involved, values for the saturation energy are necessarily ambiguous. The experiments, however, have clearly demonstrated that output energy densities as high as  $170 \text{ mJ/cm}^2$  for a 1.52-mm beam diameter (FWHM) can be achieved with the  $\text{XeF}(C \rightarrow A)$  amplifier. In order to utilize fully the broad emission band of the  $\text{XeF}(C \rightarrow A)$  amplifier to amplify short pulses, the absorption valleys in the free-running spectrum must saturate at high injection intensities, providing a smooth gain profile over the entire spectral region. Data taken at 483.2 nm, which corresponds to a strong absorption wavelength in Fig. 1, showed a single-pass gain at an injection intensity of  $25 \text{ mJ/cm}^2$  equivalent to the single-pass gain at 478.5 nm, thereby confirming saturation of the absorbers. The ASE content of the  $\text{XeF}(C \rightarrow A)$  amplifier output was less than  $10^{-5}$ .

When the injected signal was double passed through the gain region to increase the output energy further, the spatial beam profile began to change. Figure 4 depicts the evolution of the amplified beam profile, as measured with a charge-coupled device beam-imaging system, for one and two passes through the  $\text{XeF}(C \rightarrow A)$  amplifier. The spike that appears in the double-

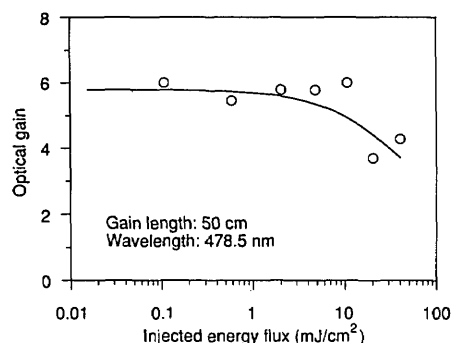


Fig. 3. Single-pass gain as a function of output energy density. Two wavelengths were probed: 478.5 nm, representing an intensity maximum in the free-running  $\text{XeF}(C \rightarrow A)$  laser, and 483.2 nm, corresponding to a strong absorption line.

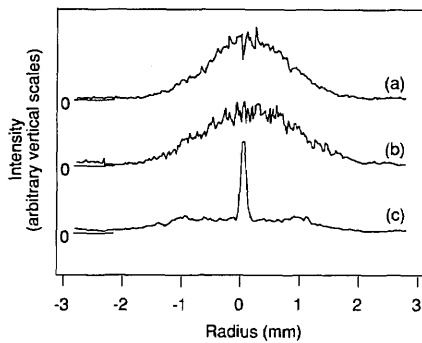


Fig. 4. Cross section of three laser beams at 478.5 nm: (a) injection dye laser, energy 0.75 mJ; (b) beam after 50-cm gain length, energy 2.9 mJ; (c) beam after 100-cm gain length, energy 3.2 mJ. The relative intensity of each curve was adjusted to fit the plotting area.

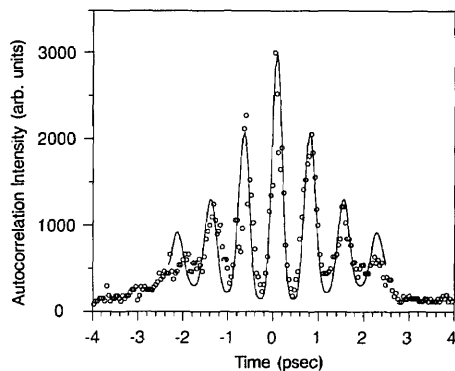


Fig. 5. Single-shot autocorrelation trace of an amplified pulse at 478.5 nm. The calculated fit (the solid curve) assumes an asymmetric pulse shape with an 800-fsec pulse duration.

passed pulse contained  $\sim 6\%$  of the pulse energy and was 10 times narrower than the initial injection pulse. It was found that this spatial narrowing occurred at approximately two times lower input energy densities when operating in a valley of the free-running XeF( $C \rightarrow A$ ) laser as opposed to a peak, suggesting that the effect may be related to the presence of saturable absorbers. In addition, the spatial narrowing appeared to occur in the gas medium rather than in the optics of the system. The 1.27-cm-thick fused silica windows were removed from the gas cell and exposed to high energy densities from the dye amplifier to check for self-focusing. At energy densities of up to  $4 \text{ J/cm}^2$ , no beam narrowing was observed; however, the windows did show self-induced absorption effects at high intensities. The intensity for the gain measurements was always low enough (below  $\sim 200 \text{ mJ/cm}^2$ ) that the window absorption was not important for the measurements reported here.

The temporal shape of the ultrashort pulses was not significantly affected during amplification. Figure 5 shows a single-shot autocorrelation of an amplified pulse at 478.5 nm with an output energy density of approximately  $40 \text{ mJ/cm}^2$ . The autocorrelator used in this experiment was similar to the one described in Ref. 16. The solid curve is a calculated fit assuming

an asymmetric exponential (1:5 rise/fall ratio) pulse shape with an 800-fsec pulse duration.<sup>12</sup> Further research in compression of the probe pulse should yield pulse durations sufficiently short to permit a measurement of the XeF rotational reorientation time and permit more detailed studies of the spectral uniformity of the gain.

The saturation energy density of the XeF( $C \rightarrow A$ ) amplifier represents an improvement of approximately 50 times in energy storage over XeCl and KrF amplifiers. In addition, the bandwidth of the XeF( $C \rightarrow A$ ) transition of  $\sim 70 \text{ nm}$  may be sufficient to amplify pulses of very short duration, such as the recently reported 10-fsec blue-green pulse produced by white-light continuum filtering.<sup>17</sup>

The authors thank the U.S. Air Force Office of Scientific Research, Office of Naval Research (Defense Advanced Research Projects Agency University Research Initiative), and the Welch Foundation for support of this research.

## References

1. P. B. Corkum and R. S. Taylor, *IEEE J. Quantum Electron.* **QE-18**, 1962 (1982).
2. S. Szatmári, B. Rácz, and F. P. Schäfer, *Opt. Commun.* **62**, 271 (1987).
3. S. Szatmári and F. P. Schäfer, *J. Opt. Soc. Am. B* **4**, 1943 (1987).
4. J. H. Glowina, G. Arjavalangan, P. P. Sorokin, and J. E. Rothenberg, *Opt. Lett.* **11**, 79 (1986).
5. A. J. Taylor, T. R. Gosnell, and J. P. Roberts, *Opt. Lett.* **15**, 118 (1990).
6. S. Watanabe, A. Endoh, M. Watanabe, N. Sarukura, and K. Hata, *J. Opt. Soc. Am. B* **6**, 1870 (1989).
7. A. P. Schwarzenbach, T. S. Luk, I. A. McIntyre, U. Johann, A. McPherson, K. Boyer, and C. K. Rhodes, *Opt. Lett.* **11**, 499 (1986).
8. P. Maine, D. Strickland, P. Bado, M. Pessot, and G. Mourou, *IEEE J. Quantum Electron.* **24**, 398 (1988).
9. C. B. Dane, S. Yamaguchi, Th. Hofmann, R. Sauerbrey, W. L. Wilson, and F. K. Tittel, *Appl. Phys. Lett.* **56**, 2604 (1990).
10. C. B. Dane, G. J. Hirst, S. Yamaguchi, Th. Hofmann, W. L. Wilson, R. Sauerbrey, F. K. Tittel, W. L. Nighan, and M. C. Fowler, "Scaling characteristics of the XeF( $C \rightarrow A$ ) excimer laser," *IEEE J. Quantum Electron.* (to be published).
11. R. Sauerbrey, W. Walter, F. K. Tittel, and W. L. Wilson, Jr., *J. Chem. Phys.* **78**, 735 (1983).
12. T. E. Sharp, C. B. Dane, F. K. Tittel, P. J. Wisoff, and G. Szabó, "A tunable, high power, subpicosecond blue-green dye laser system with a two-stage dye amplifier design," submitted to *IEEE J. Quantum Electron.*
13. A. L. Smith and P. C. Koblinsky, *J. Mol. Spectrosc.* **69**, 1 (1978).
14. L. M. Frantz and J. S. Nodvik, *J. Appl. Phys.* **34**, 2346 (1963).
15. N. Hamada, "Studies of an injection controlled rare gas halide excimer laser," Ph.D. dissertation (Rice University, Houston, Tex., 1988).
16. G. Szabó, Z. Bor, and A. Müller, *Opt. Lett.* **13**, 746 (1988).
17. R. W. Schoenlein, J. Y. Bigot, M. T. Portella, and C. V. Shank, in *Digest of Conference on Lasers and Electro-Optics* (Optical Society of America, Washington, D.C., 1990), paper PD7.